Di-urea cross-linked poly(oxyethylene)/siloxane ormolytes for lithium batteries

S. C. Nunes, V. de Zea Bermudez*

Departamento de Química and CQ-VR

Universidade de Trás-os-Montes e Alto Douro, 5000-911 Vila Real, Portugal

D. Ostrovskii

Department of Experimental Physics, Chalmers University of Technology

41296 Göteborg, Sweden

M. M. Silva, S. Barros, M. J. Smith

Departamento de Química, Universidade do Minho, Gualtar, 4710-057 *Braga, Portugal*

L. D. Carlos

Departamento de Física and CICECO, Universidade de Aveiro, 3810-193 Aveiro, Portugal

J. Rocha

Departamento de Química and CICECO, Universidade de Aveiro, 3810-193 Aveiro, Portugal

E. Morales

Instituto de Ciencia y Tecnología de Polímeros (CSIC)

Calle Juan de la Cierva 3, 28006 Madrid, Spain

Poly(oxyethylene) (POE)/siloxane hybrids (di-ureasils) doped with a wide concentration range of lithium triflate ($LiCF_3SO_3$) were investigated. The host matrix of these materials (d-U(2000)) is a sol-gel derived siliceous framework to which POE chains with about 40.5 repeat units are bonded through urea linkages. Xerogels with $\infty \geq n \geq 5$ (n is the molar ratio OCH_2CH_2/Li^+) were obtained as amorphous monoliths thermally stable up to at least 340 ºC.

* E-mail: vbermude@utad.pt

A crystalline POE/$LiCF_3SO_3$ complex was detected spectroscopically in samples with $n \leq 10$. Below 90 ºC the ormolyte with n = 20 exhibits the highest conductivity (5.8×10^{-6} $\Omega^{-1}cm^{-1}$ at 26 ºC). The redox stability domain of this material spans 4.1 V. Although FT-IR data suggest that the Li^+ ions are complexed by the POE ether oxygen atoms at $n \leq 10$, this threshold composition is probably located at slightly lower salt content. "Free" triflate ions and weakly coordinated anions, present in all the samples examined, must be the main charge carriers of the d-$U(2000)_{20}LiCF_3SO_3$ xerogel. Ion pairs ($Li^+CF_3SO_3^-$) or negatively charged triplets ($[Li(CF_3SO_3)_2]^-$) are formed at $n \leq 40$. At $n \leq 5$ positively charged triplets $[Li_2(CF_3SO_3)]^+$ also appear. Divalent positively charged multiplets $[Li_3(CF_3SO_3)]^{2+}$ occur at n = 1.

Introduction

A long-standing objective of research within the domain of solid-state electrochemistry has been the synthesis of polymer electrolytes[1,2] that combine the physical properties of conventional thermoplastics with the high ionic conductivity required in applications such as high energy density batteries.[3]

Polymer electrolytes are prepared through the dissolution of an ionic salt in an adequate polymer. The host polymer is typically a polyether, such as POE, a macromolecule that displays a remarkable solvating ability towards cations. The Li^+-based polymer systems have yielded the highest conductivities reported to date and thus have been the most widely investigated.[4]

The practical application of POE-based electrolytes in solid state electrochemical devices has been somewhat delayed, however, by their poor processability and marked tendency to crystallise. In 1983, Berthier et al.[5] provided conclusive evidence that in semi-crystalline polymer electrolyte systems the ionic conductivity is confined to amorphous regions. This suggested that high ionic conductivity should be correlated with polymer matrices that had

low glass transition temperatures (T_g). This view prevailed in the polymer electrolyte research community until Gadjourova et al.[6] demonstrated very recently that ionic conductivity in the crystalline domains of the matrix can be significantly higher than in the corresponding amorphous phases. As the low levels of conductivity exhibited by the complexes described by Gadjourova et al.[6] do not permit to foresee their immediate application as practical electrolytes, a considerable amount of the research currently carried out is still focused on the development of amorphous systems.

Organically modified silicate electrolytes (*ormolytes*) represent a valuable alternative to conventional polymer electrolytes. The ormolyte concept relies on the production of sol-gel[7] derived organic/inorganic host frameworks[8] that are able to accommodate the ionic species: while the organic component includes the solvating POE segments, the inorganic component is a siloxane network. In these materials crystallinity is either significantly reduced or completely suppressed and extremely high contents of salt may be incorporated without any undesirable consequences. In addition, samples of these materials may be readily processed into thin films or monoliths and a marked improvement in the mechanical resistance and chemical/thermal stability results. The organic/inorganic hybrid strategy has been successfully employed in the last few years to prepare several Li^+-doped ormolytes. [9-16]

The present work is focused on the investigation of the structure, morphology, thermal properties and electrochemical behaviour of a series of POE/siloxane ormolytes containing a wide range of $LiCF_3SO_3$ concentration. The host structure of the materials analysed belongs to the class of *di-ureasils*,[17-19] a family of hybrids in which the organic and inorganic components are bonded through urea groups. The di-ureasil matrix employed, which possesses approximately 40.5 oxyethylene repeat units per polymer segment, was chosen because of the encouraging conductivities displayed by electrolytes based on this host matrix doped with Eu^{3+} ions.[20,21] In an attempt to understand the ionic conductivity mechanism, we

have used vibrational spectroscopy to examine the cation/polymer and cation/anion interactions.

Experimental

Starting Materials - Lithium trifluoromethanesulfonate ($LiCF_3SO_3$, Aldrich) and α,β-diaminepoly(oxyethylene-co-oxypropylene (commercially designated by Jeffamine ED-2001®, Fluka, average molecular weight 2001 g/mol) were dried under vacuum at 25 ºC for several days prior to being used. 3-isocyanatepropyltrietoxisilane (ICPTES, Fluka) was used as received. Ethanol (CH_3CH_2OH, Merck) and tetrahydrofuran (THF, Merck) were stored over molecular sieves. High purity distilled water was used in all experiments.

Synthesis of the di-ureasils - The preliminary stage of the preparation of Li^+-doped di-ureasils involved the formation of a covalent bond between the terminal NH_2 groups of Jeffamine-2001® and the -N=C=O group of ICPTES in THF to yield the urea cross-linked organic-inorganic hybrid precursor designated as di-ureapropyltriethoxysilane (d-UPTES(2000)). The grafting process was infrared monitored. During the formation of the urea groups the intensity of the strong and sharp band characteristic of the stretching vibration of the -N=C=O group of ICPTES, typically located at 2273 cm^{-1}, was progressively reduced, until it disappeared upon completion of the reaction. In parallel, a series of new bands, associated with the vibrations of the urea group, appeared in the 1760-1530 cm^{-1} spectral region. The d-UPTES(2000) compound was produced as a transparent oil. Its structure, represented in Scheme 1, was confirmed by ^1H NMR ($CDCl_3$, 400.13 MHz) and ^{13}C NMR ($CDCl_3$, 100.62 MHz) (Table 1).

In the second stage of the synthetic procedure, a mixture of CH_3CH_2OH and water was added to the d-UPTES(2000) solution, followed by the incorporation of $LiCF_3SO_3$. Samples with n = ∞, 200, 100, 80, 60, 40, 20, 10, 7, 5 and 1 were prepared according to the procedure described elsewhere[20,21]. Details of the synthesis of the d-$U(2000)_nLiCF_3SO_3$ xerogels are

indicated in Table 2. The samples with n > 1 were obtained as transparent, flexible monoliths with a yellowish hue. The d-U(2000)$_1$LiCF$_3$SO$_3$ material was produced as a white solid.

In agreement with the terminology used in previous papers[20,21], the hybrid matrix of the materials obtained was designated as d-U(2000), where d indicates di, U denotes the urea group and 2000 corresponds to the average molecular weight of the starting organic precursor. The di-ureasils doped with $LiCF_3SO_3$ will be described by the d-U(2000)$_n$LiCF$_3$SO$_3$ notation, where n (salt composition) represents the number of ether oxygen atoms per Li^+ cation. For instance, the xerogel material d-U(2000)$_{80}$LiCF$_3$SO$_3$ is the di-ureasil incorporating an amount of $LiCF_3SO_3$ such that the O_{POE} / Li^+ ratio is equal to 80.

Experimental Techniques. - The ^{1}H and ^{13}C NMR spectra were recorded in $CDCl_3$ on a Brüker ARX400 NMR spectrometer (400.13 MHz and 100.62 MHz, respectively) at CACTI-Universidad de Vigo (Spain). Chemical shifts, δ, are quoted in ppm from tetramethylsilane (TMS).

^{29}Si magic-angle spinning (MAS) and ^{13}C cross-polarization (CP) MAS NMR spectra were recorded on a Brüker Avance 400 (9.4 T) spectrometer at 79.49 and 100.62 MHz, respectively. ^{29}Si MAS NMR spectra were recorded with 2 s (equivalent to 30 º) rf pulses, a recycle delay of 60 s and at a 5.0 kHz spinning rate. ^{13}C CP/MAS NMR spectra were recorded with 4 s ^{1}H 90º pulse, 2 ms contact time, a recycle delay of 4 s and at a spinning rate of 4.5 kHz (the spinning rate of the ^{13}C CP/MAS NMR spectrum for the undoped sample is 8.kHz). Chemical shifts are quoted in ppm from TMS.

The X-ray diffraction (XRD) measurements were performed at room temperature (RT) with a Rigaku Geigerflex D/max-c diffractometer system using monochromated CuK_α radiation (λ = 1.54 Å) over the 2θ range of between 4 and 80º at a resolution of 0.05º. The xerogel samples, analyzed as films, were not submitted to any thermal pre-treatment.

A DSC131 Setaram Differential Scanning Calorimeter was used to determine the thermal characteristics of the ormolytes. Disk sections with masses of approximately 30 mg were removed from the di-ureasil film, placed in 40 μl aluminium cans and stored in a dessicator over phosphorous pentoxide (P_2O_5) for one week at RT under vacuum. In the case of the di-ureasils with n = 5 and 1 it was necessary to grind the samples first to form a fine powder in order to remove all the water. After this drying treatment the cans were hermetically sealed and the thermograms were recorded. Each sample was heated from 25 to 300 ºC at 10 ºC min^{-1}. It was subsequently quenched from RT to -100 ºC and then heated up to 80 ºC at 15 ºC min^{-1}. The purge gas used in both experiments was high purity nitrogen supplied at a constant 35 cm^3 min^{-1} flow rate. Samples for thermogravimetric studies were transferred to open platinum crucibles and analysed using a Rheometric Scientific TG 1000 thermobalance at a heating rate of 10º min^{-1} using dried nitrogen as purging gas (20 ml/min). Prior to measurement, the xerogels were vacuum-dried at 80 ºC for about 48 h and kept in an argon-filled glove box.

For bulk conductivity measurements, an ormolyte disk was placed between two 10 mm diameter ion-blocking gold electrodes (Goodfellow, > 99.9%). The electrode/ormolyte/electrode assembly was secured in a suitable constant volume support. The cell support was installed in a Buchi TO51 tube oven and a type K thermocouple placed close to the electrolyte disk measured the sample temperature. Bulk conductivities of the samples were obtained during heating cycles using the complex plane impedance technique (Schlumberger Solartron 1250 frequency response analyser and 1286 electrochemical interface) over a temperature range of between 25 and 100 ºC and at approximately 7 ºC intervals. Prior to recording the thermograms, the di-ureasil ormolytes were vacuum-dried at 80 ºC for about 48h and kept in an argon-filled glove box.

The electrochemical stability of the solid polymer electrolytes was examined by means of cyclic voltammetry using Radiometer/Copenhagen Voltalab 32 potentiostat/galvanostat equipment. A stainless steel working electrode was used with lithium foil counter and

reference electrodes. Swagelok type test cells (6 mm diameter) were assembled and sealed in an argon-filled glove box. Prior to characterization, the ormolyte sample was dried under vacuum at 60 ºC for about 24 hours. Experiments were run at RT at a sweep rate of 10 mV/s.

FT-IR spectra were acquired at RT using a Bruker 22 (Vektor) spectrometer placed inside a glove-box with a dry argon atmosphere. The spectra were collected over the 4000-400 cm^{-1} range by averaging 150 scans at a spectral resolution of 2 cm^{-1}. Solid samples (2 mg) were finely ground, mixed with approximately 175 mg of dried potassium bromide (Merck, spectroscopic grade) and pressed into pellets. Prior to recording the spectra, the pellets were first vacuum dried at 80-90 ºC for about 60 h, in order to reduce the levels of adsorbed water and solvent, and then transferred into a glove-box.

The FT-Raman spectra were recorded at RT with a Bruker IFS-66 spectrometer equipped with a FRA-106 Raman module and a near-infrared YAG laser with wavelength 1064 nm. The spectra were collected over the 3200-300 cm^{-1} range at a resolution of 2 cm^{-1}. The accumulation time for each spectrum was 4 hours.

To evaluate complex band envelopes and to identify underlying spectral components, the iterative least-squares curve-fitting procedure in the PeakFit[22] software was used extensively throughout this study. The best fit of the experimental data was obtained by varying the frequency, bandwidth and intensity of the bands. Taking into account the morphology of materials under investigation we decided to employ Gaussian band shapes. It is well known that the disordering of a system, which causes statistical distribution of the oscillators, may explain why the experimentally observed band shapes are very often changed from the natural Lorentzian shape toward the Gaussian form. As a consequence, typical band profiles observed in solid disordered materials (e.g., polymers, glasses and non-ideal crystals) are rather Gaussian. Although it is in general accepted that in such cases the peaks are best fitted with a Voigt shape (a mixture of Lorentzian and Gaussian contributions), the use of this function is

not straightforward and may lead to ambiguous results due to the possibility of different Gaussian-Lorentzian proportions.

Results and Discussion

Structure, morphology and thermal properties of the d-U(2000)$_n$LiCF$_3$SO$_3$ ormolytes - Figs. 1(a) and 1(b) show the ^{13}C CP/MAS and ^{29}Si MAS NMR spectra of representative samples of the d-U(2000)$_n$LiCF$_3$SO$_3$ di-ureasil family, respectively. The position δ and assignment[11,23-31] of the resonance peaks are given in Table 1.

Fig. 1(a) demonstrates that the ^{13}C CP/MAS NMR spectra of the di-ureasils with n = ∞, 80, 10 and 7 are dominated by a prominent peak centered around 70 ppm, associated with the resonance of the oxyethylene CH_2 carbon atoms (Table 1). Because of the high concentration of these moieties in d-U(2000), the signals associated with the carbon atoms of all the other functional groups present in this hybrid matrix are relatively weak. As the salt concentration increases, there is a broadening of the signal at *ca.* 70 ppm, its full width at half maximum being 29 and 39 Hz at n = 80 and 10, respectively (Fig. 1(a)). As it will be demonstrated below, in the d-U(2000)$_{80}$LiCF$_3$ sample the Li^+ ions do not interact with the ether oxygen atoms.

Comparison of the ^{13}C CP/MAS NMR spectra of the d-U(2000)$_n$LiCF$_3$SO$_3$ xerogels with that of the d-UPTES(2000) precursor compound confirms that no modifications of the Si-bonded propyl chains, urea groups or oxyethylene/oxypropylene moieties occurred during the second stage of the synthetic procedure of the di-ureasil composites (Table 1). There are, however, indications (see carbon atoms C^4 and C^5 in Table 1) that non-reacted OCH_2CH_3 groups remain in the non-doped and doped materials, a result that clearly suggests that the hydrolysis reaction did not continue to completion.

In the ^{29}Si MAS NMR spectra of the di-ureasils with n = 80, 20 and 10 three signals are detected at approximately -50.7, -57.6 and -66.1 ppm (Fig. 1(b)). Based on the conventional

T_m silicon notation (m = 1, 2 and 3, where m is the number of silicon-bridging oxygen atoms**), these peaks are attributed to T_1, T_2 and T_3 units, respectively (Table 1). The relative proportions determined for these different silicon environments (Table 1) show that in this set of samples the main site present is T_3, usually associated with CH_2-Si(OSi)$_3$ moieties, a result that supports the suggestion that the condensation process favoured branched structures rather than linear segments. The polycondensation rates c (where c = 1/3 ($\%T_1 + 2\%T_2 + 3\%T_3$)) calculated for the Li^+-doped di-ureasils examined by ^{29}Si MAS NMR demonstrate that the highest polycondensation degree was reached in the case of the most dilute sample (Table 1). The value exhibited by d-U(2000)$_{10}$LiCF$_3$SO$_3$ is similar to that displayed by the non-doped framework.[32] The empirical formula derived from the ^{29}Si MAS NMR data for each of the samples analyzed (Table 1) corroborate the conclusion drawn from the ^{13}C CP/MAS NMR spectra that in the final materials a minor number of ethoxy (and very likely hydroxyl) groups persist bonded to the silicon atoms.

The diffractograms of the d-U(2000)$_n$LiCF$_3$SO$_3$ di-ureasil xerogels reproduced in Fig. 2 indicate that the samples with $200 \geq n > 1$ are totally amorphous. This result proves that the addition of the guest lithium salt to d-U(2000) inhibits the formation of crystalline phases of free LiCF$_3$SO$_3$, POE/salt complexes or pure POE. The existence of crystalline POE chains in the non-doped hybrid is responsible for the sharp and intense Bragg peaks discerned at about 19.15 and 23.25º in the XRD pattern of d-U(2000) (Fig. 2).[33] The broad band, Gaussian in shape, located at approximately 21.61º in the XRD patterns of the di-ureasils with $200 \geq n \geq 5$ is ascribed to the coherent diffraction of the siliceous domains.[33] The structural unit distance, calculated using the Bragg law, is approximately 4.22 Å. The weak broad hump distinguished at ca. 40º in the diffractogram of d-U(2000)$_5$LiCF$_3$SO$_3$ might be associated with the second-order of the peak centered near 21.61º (Fig. 2). These findings confirm that the use of the

** The classical notation T_n has been changed to T_m, to avoid any confusion with the notation n used throughout the text to designate salt composition.

siloxane-modified POE structure instead of linear POE is clearly beneficial. In fact, the phase diagram of the $POE_nLiCF_3SO_3$ system exhibits various crystalline domains in this concentration range at RT.[34-36]

In the case of the salt-rich material d-$U(2000)_1LiCF_3SO_3$, a series of peaks centered at about 10.52, 12.46, 17.92, 19.80, 20.76, 21.38, 24.76, 25.76, 26.72, 28.08, 28.74 and 33.90 º are detected (Fig. 2). The absence of the reflections characteristic of the salt bear witness to the inexistence of free $LiCF_3SO_3$ in this ormolyte. As the position of these peaks coincides exactly with the location of the diffraction peaks of the crystalline complex with stoichiometry 3:1[35,37] that is formed between high molecular weight POE and $LiCF_3SO_3$,[38] we may presume that this complex also appears in the d-U(2000) medium at n = 1.

The DSC curves of the d-$U(2000)_nLiCF_3SO_3$ xerogels in the 20-300 ºC range are represented in Fig. 3(a). The thermogram of d-U(2000) exhibits a melting peak centered at 40 ºC (Fig. 3(a)), ascribed to the fusion of crystallites of POE, thus confirming the semi-crystalline character of this material suggested by XRD data. The inspection of the DSC curves of the $LiCF_3SO_3$-doped di-ureasils with $n \geq 5$ allows us to deduce that the incorporation of increasing amounts of the guest lithium salt into the host organic/inorganic matrix produces entirely amorphous xerogels in this range of salt content (Fig. 3(a)). Upon further addition of $LiCF_3SO_3$ to d-U(2000) (n = 1) a single endothermic, broad and very intense event is produced (Fig. 3(a)). This peak, centered at about 154 ºC (onset at approximately 123 ºC), is attributed to the fusion of the POE-based complex with n = 3 identified by means of XRD. This melting temperature is considerably lower than that reported for the $POE_3LiCF_3SO_3$ electrolyte (172 ºC),[36] an expected result since the POE chains included in d-U(2000) are significantly shorter than those of the high molecular weight POE employed by Vallée et al.[36]. The pair of endotherms characteristic of the free salt centered near 62 and 141 ºC, assigned to the loss of hydration water molecules, are not

detected in the DSC trace of the most concentrated samples (Fig. 3(a)). We note that $LiCF_3SO_3$ melts at ca. 430 ºC.[36]

When dealing with sol-gel derived materials broad endotherms, usually centered around 100 ºC, are often observed in the thermograms. No such features, normally ascribed to the evaporation of occluded solvents (water, ethanol or THF), are discerned in any of the thermograms depicted in Fig. 3(a)). Samples submitted to DSC measurements were previously stored in a dessicator over P_2O_5 for one week at RT under vacuum (see Experimental section). It is useful to mention at this stage that the d-U(2000) matrix is only slightly hygroscopic. This implies that in the Li^+-doped samples the presence of water must be exclusively associated with the guest lithium salt, owing to the markedly hygroscopic nature of the Li^+ species. Nevertheless, the almost complete removal of water from the salt-containing materials could be readily accomplished by drying under vacuum at RT, in the presence of a dessicant, as confirmed by the low intensity of the characteristic broad OH stretching envelope in the high-frequency region of the FT-IR spectra (not shown).

The variation of the T_g of the d-U(2000)$_n$$LiCF_3SO_3$ di-ureasils with composition is reproduced in Fig. 3(b). The determination of the T_g is fundamental in the context of polymer electrolytes. In these systems, the cation/polymer interaction is accompanied by the formation of transient ionic cross-links that partially restrict the local motion of the adjacent solvating segments.[3] This effect typically leads to the upshift of the T_g of the host polymer. In the plot of Fig. 3(b) we observe that the T_gs of samples with $n > 20$ are essentially the same as that of d-U(2000) (-54 ºC). In contrast, in xerogels with $n \leq 20$ the T_g of the POE segments suffers a significant increase with salt addition (Fig. 3(b)), an indication that Li^+/polymer bonding takes place in these materials. The marked increase of T_g at high salt concentration is noteworthy (37 ºC at $n = 1$). These results induce us to envisage two possible scenarios for the Li^+ ion coordination in the dilute xerogels with $n > 20$: (1) the POE chains of d-U(2000) are not involved in the complexation of the alkali metal cations; (2) in this range of salt composition

the number of Li^+/POE interactions is too low to influence the T_g of the sample. We will return to the discussion of this fundamental aspect in the section devoted to the spectroscopic analysis of the cation/polymer interactions.

The TGA curves of selected Li^+-based di-ureasils shown in Fig. 3(c) lend support to the observation that the presence of the guest lithium salt appears to stabilise the hybrid host structure in a non-oxidising atmosphere. In all the samples analysed a unique mass loss is detected in the curves (Fig. 3(c)). While in the xerogels with $n = \infty$, 80 and 40 thermal decomposition starts near 305, 338 and 347 ºC, respectively, the compounds with $20 \geq n \geq 7$ are thermally stable up to approximately 384 ºC (Fig. 3(c)). The degradation of d-$U(2000)_5LiCF_3SO_3$ is initiated at about 370 ºC (Fig. 3(c)).

Electrochemical behaviour of the d-U(2000)$_n$LiCF$_3$SO$_3$ electrolytes - The analysis of the Arrhenius conductivity plots of the d-$U(2000)_nLiCF_3SO_3$ ormolytes with $\infty > n \geq 5$ depicted in Fig. 4(a) leads us to the conclusion that some of these materials exhibit moderate ionic conductivity over the range of temperatures considered. At temperatures lower than 90 ºC, d-$U(2000)_{20}LiCF_3SO_3$ is the most conducting sample of the whole series of di-ureasils investigated (e.g., approximately 5.8×10^{-6} $\Omega^{-1}cm^{-1}$ at 26 ºC).

The conductivity isotherms included in Fig. 4(b) show the presence of two conductivity maxima: one appears at n = 20 (see inset of Fig.4(b)) and the second, considerably less pronounced, is apparent at n = 100. At temperatures greater than 90 ºC, the high concentration maximum shifts to n = 10. These findings are in perfect agreement with the results of Robitaille and Fauteux[34] who reported the presence of two conductivity maxima at n = 100 and 18 in the $POE_nLiCF_3SO_3$ system at temperatures greater than 60 ºC. The latter temperature corresponds to the melting temperature of the eutectic located around n = 100 in the phase diagram.[34]

The low conductivity observed in the xerogel with n = 5 (Fig. 4(a)) over the whole range of temperatures is associated with the formation of the crystalline $POE_3LiCF_3SO_3$ complex. It is worth referring in this context that below 55 ºC d-U(2000) is more conducting than d-$U(2000)_5LiCF_3SO_3$ (Fig. 4(a)). The moderate conductivity exhibited by this essentially amorphous, non-doped hybrid structure between 25 and 100 ºC (approximately $1x10^{-8}$ to $2x10^{-7}$ $\Omega^{-1}cm^{-1}$, respectively (Fig. 4(a)) was correlated with proton hopping between neighbouring urea groups.[18]

According to the ^{29}Si MAS NMR data, a minor proportion of non-reacted, low molecular weight precursor molecules remain in the final xerogels. However, as their concentration is very low, these species are not expected to influence the conductivity of the ormolyte samples.

It is of interest to compare the values of ionic conductivity observed for the d-$U(2000)_nLiCF_3SO_3$ composites with those of the $POE_nLiCF_3SO_3$ family. Due to the high proportion of crystalline material, the POE-based electrolytes are typically poor conductors at ambient temperature. The Arrhenius plots of Fig. 4(a) prove that the sol-gel strategy permits this problem to be resolved. At 30 ºC the most conducting $POE_nLiCF_3SO_3$ samples exhibit conductivity values around 10^{-7} $\Omega^{-1}cm^{-1}$,[34] whereas at the same temperature the conductivity of the di-ureasil compounds with $100 \geq n \geq 7$ varies from 10^{-6} to 10^{-5} $\Omega^{-1}cm^{-1}$ (Fig. 4(a)). As expected, at higher temperatures the electrolytes produced using POE as host polymer are better ionic conductors than the analogues derived from the d-U(2000) host hybrid framework. While the $POE_{100}LiCF_3SO_3$ and $POE_{20}LiCF_3SO_3$ electrolytes exhibit conductivities around 10^{-3} $\Omega^{-1}cm^{-1}$ at 111 ºC,[34] the most conducting ormolyte sample (n = 10) displays a conductivity of about $2.1x10^{-4}$ $\Omega^{-1}cm^{-1}$ at 103 ºC (Fig. 4(a)).

Early studies confirmed that the use of $LiCF_3SO_3$ in POE-based polymer electrolytes for secondary batteries is not viable.[39] In contrast, the triflate ion may be safely employed in

primary batteries, as the insoluble layer of LiF formed protects the lithium metal electrode.[39] In the voltammogram of $POE_{4.5}LiCF_3SO_3$ the cathodic peaks at -2.8 and -1.7 V vs. Ag/Ag_3SI (+1.05 and +2.15 V vs. Li/Li^+, respectively), characteristic of lithium deposition and triflate reduction, respectively, and the anodic oxidation of the anion at +2.4 V vs. Ag/Ag_3SI (+6.25 V vs. Li/Li^+) allow us to affirm that the redox stability domain of this electrolyte spans 4.1 V.[39]

The results of the cyclic voltammetry performed at RT on the amorphous d-$U(2000)_{20}LiCF_3SO_3$ composite, a conductivity maximum of this di-ureasil system, are reproduced in Fig. 5. The ormolyte stability is demonstrated by the negligibly small currents observed at extreme potentials (e.g., 9.1 A/cm^2 at 5 V vs. Li/Li^+) (Fig. 5).

Cation/polymer and cation/anion interactions - In polymer electrolytes several types of charge carriers may participate in the conduction process: (a) "free" or weakly coordinated ions with relatively high mobility; (b) cations interacting strongly with the host polymer and thus with low mobility; (c) charged aggregates with moderate to low mobility. Papke et al.[40] established that in POE-based electrolytes containing monovalent ions an increase in the number of uncharged ion pairs is accompanied by a decrease in the ionic conductivity.

Infrared and Raman spectroscopies are powerful tools in the elucidation of the ionic conductivity/ionic association relationship in polymer electrolyte systems. This sort of spectroscopic analysis usually involves the examination of diagnostic bands of the host polymer and of the anion. In the present work we chose to incorporate the Li^+ ions as a triflate salt, since the $CF_3SO_3^-$ ion probe has vibration modes that are easily identified in the infrared and Raman spectra and whose attribution is well documented.

To examine the coordination of the Li^+ ions to the POE chains we decided to inspect the skeleton CO stretching (νCO) mode of the spectra of the di-ureasil ormolytes, as this mode is very sensitive to alterations of the backbone conformation arising from the cation/ether oxygen atom interaction.

The RT FT-IR spectra of selected d-U(2000)$_n$LiCF$_3$SO$_3$ compounds in the νCO region (1200-1060 cm^{-1}) are presented in Fig. 6(a). The curve-fitting results of the spectra of representative samples in this range of wavenumbers are shown in Figs. 6(b) and 6(c).

In the νCO region the complexation of the Li^+ ions by the oxygen atoms of the POE chains induces a distinct shift of the prominent νCO band to 1095-1089 cm^{-1} .[41,42] The FT-IR spectrum of d-U(2000) displays in this spectral region an intense broad band around 1111 cm^{-1} and a shoulder at about 1148 cm^{-1} (Fig. 6(b)), ascribed to the νCO vibration mode and to the coupled vibration of the νCO and rCH$_2$ modes, respectively.[43,44] The intensity and frequency of both features persists essentially unchanged within the 200 ≥ n ≥ 20 salt composition range (Fig. 6(b)). As these spectral events are characteristic of non-coordinated, disordered oxyethylene moieties,[43,44] we may deduce, not only that in the di-ureasil samples with n ≥ 20 the ether oxygen atoms of the polymer segments do not in principle bond to the monovalent alkali metal cations, but also that these POE chains remain amorphous over the same concentration interval. The latter conclusion is consistent with the XRD and DSC data. The further incorporation of guest triflate salt into d-U(2000) (n = 10) gives rise to the appearance of new components in the broad νCO band (Fig. 6(c)): although the polymer features located at 1148 and 1111 cm^{-1} subsist, three new events appear at 1162, 1137 and 1090 cm^{-1} and two new shoulders emerge around 1175 and 1080 cm^{-1}. In the salt-rich sample with n = 5 the νCO envelope suffers major modifications (Fig. 6(c)): the band profile becomes better resolved, with strong bands located at 1162, 1111 and 1090 cm^{-1}. The 1175 and 1162 cm^{-1} bands - attributed to the asymmetric stretching vibration of the CF_3 group - and the 1137, 1090 and 1080 cm^{-1} features coincide exactly with those produced by the POE$_3$LiCF$_3$SO$_3$ crystalline complex,[45] thus providing evidence of the occurrence of this compound in the d-U(2000)$_{10}$LiCF$_3$SO$_3$ and U(2000)$_5$LiCF$_3$SO$_3$ materials. Nevertheless, the presence of the 1111 cm^{-1} band in the spectra of both composites gives support to the explanation that non-

coordinated and amorphous POE chains coexist with the crystalline compound at n = 10 and 5. Curiously, the POE/$LiCF_3SO_3$ complex is only detected at n = 1 by XRD (Fig. 2) and DSC (Fig. 3(a)).

Although the first spectroscopic signs of Li^+/POE bonding are evident in the νCO region at n = 10, the salt concentration at which the alkali metal cations start to effectively interact with the ether oxygen atoms of the polymer chains may be lower. In fact, in the case of the more dilute di-ureasil samples (n > 10) it is very likely that the broad and strong νCO envelope centred at 1111 cm^{-1} (Fig. 6(a)) is masking the characteristic band of Li^+-coordinated amorphous POE chains. Interestingly, the changes detected in the CH_2 rocking region of the same set of samples indicate that the complexation of the alkali metal cations by the ether oxygen atoms of POE is initiated at n = 20,[46] thus as a slightly higher value of n (lower salt concentration) than that indicated by analysis of the νCO region.

Neither the results of thermal analysis, nor spectroscopic data, allow us to determine with certainty the composition that corresponds to the beginning of PEO chain participation in the cation coordination in the d-U(2000)$_n$$LiCF_3SO_3$ composites. Given that there are two different types of sites in the host matrix where complexation may occur (the ether oxygen atoms of the POE chains and the carbonyl oxygen atoms of the urea linkages), it seems plausible that at low salt concentrations the site with lower energy is occupied preferentially. Under these conditions the POE chains of d-U(2000) may not be involved in the coordination of alkali metal cations until a certain critical electrolyte composition is reached. According to the results of the analysis of the "amide I" region of the same set of di-ureasil materials,[46] the Li^+ ions bond to the urea carbonyl oxygen atoms in all the samples studied here.

The triflate oxygen atoms are the third type of coordinating site available for the Li^+ ions in the d-U(2000)$_n$$LiCF_3SO_3$ xerogels. Let us now assess the nature and extent of ion pairing and ion aggregation in the lithium-doped di-ureasils as a function of $LiCF_3SO_3$ concentration.

We will examine for this purpose two diagnostic vibration modes of the triflate ion which are very sensitive to coordination effects: the symmetric stretching vibration of the SO_3 group (ν_sSO_3) and the symmetric deformation of the CF_3 group (δ_sCF_3).

ν_sSO_3 region: The ν_sSO_3 mode of a "free" triflate ion gives rise to a feature located at 1032 cm^{-1}.[47] Upon coordination to the Li^+ ion, the ν_sSO_3 band - associated with a non-degenerate mode of the $CF_3SO_3^-$ ion - is shifted to higher wavenumbers.[42, 45,48-58]

The FT-Raman spectra of selected di-ureasils in the ν_sSO_3 region and the results of the curve-fitting performed in the ν_sSO_3 envelope are represented in Figs. 7(a) and 7(b), respectively.

The ν_sSO_3 band of the FT-Raman spectra of the xerogels with $n \geq 7$ was decomposed into four components: a sharp band at 1032 cm^{-1}, two weak shoulders positioned around 1039 and 1025 cm^{-1} and a very weak, ill-defined peak centered around 1045 cm^{-1} (Fig. 7(b)). In this range of salt composition the 1032 cm^{-1} feature is considerably stronger than the shoulders, although the introduction of increasing amounts of lithium salt leads to a moderate increase of the intensity of the 1045 and 1039 cm^{-1} features (Fig. 7(b)). A marked reduction of the intensity of the 1025 cm^{-1} shoulder occurs in parallel (Fig. 7(b)). In the FT-Raman spectrum of the rich-salt sample with n = 5 several changes are worth noting: although the 1032 cm^{-1} event subsists as the strongest band of this spectral region, the 1025 cm^{-1} is no longer seen, the components at 1045 and 1039 cm^{-1} become significantly more intense and a new shoulder located at about 1052 cm^{-1} is discerned (Fig. 7(b)). The FT-Raman profile of the ν_sSO_3 band of the most concentrated hybrid studied (n = 1) was best fitted with five peaks centered at 1063, 1052, 1045, 1039 and 1032 cm^{-1} (Fig. 7(b)). The strongest component is the one situated at 1052 cm^{-1}, followed by those at 1045, 1039 and 1032 cm^{-1} (Fig. 7(b)).

The presence of the 1032 cm^{-1} band in the FT- Raman spectra of all the doped di-ureasil xerogels inspected unequivocally confirms the occurrence of "free" anions over the whole

range of salt concentration. We cannot, however, discard the contribution to the 1032 cm^{-1} band of the so-called "cross-link separated ion pairs", as observed in analogue materials.[59-61] This would explain the regular increase of this feature as $LiCF_3SO_3$ concentration is progressively increased and specially its remarkable intensity at n = 1. The shoulders found at 1039 and 1025 cm^{-1} are associated with weakly coordinated triflate ions located in two different sites: (1) $CF_3SO_3^-$ species weakly bonded to Li^+ ions, which simultaneously interact with the carbonyl oxygen atoms of the urea groups; (2) $CF_3SO_3^-$ ions hydrogen-bonded to the urea N-H groups.[59] The feature situated near 1045 cm^{-1} in samples with $n \leq 40$ is attributed to the formation of monodentate $Li^+CF_3SO_3^-$ ions pairs or negatively charged triplets $[Li(CF_3SO_3)_2]^-$.[49,51,53] The component seen near 1052 cm^{-1} in the spectra of the di-ureasils with n = 5 and 1 is ascribed to the existence of a bidentate bridging aggregate (aggregate I)[49] (the positively charged triplet $[Li_2(CF_3SO_3)]^+$)[49,51,53]. This result correlates well with the detection of the $POE_3LiCF_3SO_3$ crystalline complex[37,57,58] at n = 5 and 1. In fact in this compound the triflate ion vibrates essentially as the $[Li_2(CF_3SO_3)]^+$ entity because two oxygen atoms of the $CF_3SO_3^-$ ion bridge, in a monodentate arrangement, two Li^+ ions that lie adjacent to each other within the polymer helix.[37,57,58] At last, the event that emerges at 1063 cm^{-1} in the ν_aSO_3 region of the most concentrated di-ureasil prepared is associated with the presence of a tridentate bridging aggregate (aggregate II)[49], the divalent positively charged multiplet $[Li_3(CF_3SO_3)]^{2+}$. The absence of a band at 1077 cm^{-1} in the ν_aSO_3 envelope of any of the samples analyzed excludes the occurrence of pure crystalline salt[54] and therefore confirms the XRD and DSC results. The anionic configurations detected in the FT-Raman SO_3 symmetric stretching region are in perfect agreement with those deduced from the FT-IR spectra.[46]

δ_sCF_3 region: Several authors consider that the δ_sCF_3 mode is a much more reliable way of identifying $CF_3SO_3^-$ ions in different coordinating environments than the ν_sSO_3 mode.

[37,42,45,49,57,58] The $\delta_s CF_3$ vibration is located near 754 cm^{-1} when the ion is "free".[50] Shifts to higher wavenumbers result upon interaction of this anion with the Li^+ ion.[37,42,45,49,57,58]

The FT-Raman spectra of selected Li^+-doped di-ureasils in the $\delta_s CF_3$ region and the results of the tentative curve-fitting carried out in the $\delta_s CF_3$ envelope are represented in Figs. 8(a) and 8(b), respectively.

While the $\delta_s CF_3$ band of the material with n = 40 was resolved into a pair of components situated at about 754 and 757 cm^{-1}, at higher salt concentration ($20 \geq n \geq 5$) the band contour was best fitted with an additional peak at 762 cm^{-1} that grows with salt addition (Fig. 8(b)). We note in this range of compositions the marked decrease of the intensity of the 754 cm^{-1} component (Fig. 8(b)). The $\delta_s CF_3$ band of the salt-rich di-ureasil with n = 1 was decomposed into a prominent band at 766 cm^{-1} and a minor component at 762 cm^{-1} (Fig. 8(b)).

Based on the attribution of Huang et al.,[49] the 754, 757, 762 and 766 cm^{-1} components discerned in the FT-Raman spectra of the d-U(2000)$_n$$LiCF_3SO_3$ composites are associated with the following entities, respectively: "free" triflate ions, $Li^+CF_3SO_3^-$ ion pairs (or $[Li(CF_3SO_3)_2]^-$ triplets), aggregate I ($[Li_2(CF_3SO_3)]^+$) and aggregate II ($[Li_3(CF_3SO_3)]^{2+}$). As mentioned above, these species are manifested in the $\nu_s SO_3$ region as bands situated at 1032, 1045, 1052 and 1063 cm^{-1}, respectively.[49]

Comparison of the curve-fitting data obtained for the $\nu_s SO_3$ (Fig. 7(b)) and $\delta_s CF_3$ (Fig. 8(b)) regions leads us to the conclusion that there is not a direct correspondence between the number of resolved components. For instance, in the case of the sample with n = 1, the $\delta_s CF_3$ band results essentially from the presence of aggregates II (Fig. 8(b)), unlike the corresponding $\nu_s SO_3$ envelope that demonstrates the occurrence of four different coordinating environments for the triflate ion (Fig. 7(b)). This evidence may be correlated with the fact that the CF_3 end of the triflate ion in the di-ureasils is apparently significantly less perturbed by ion association than the SO_3 end. This is not unexpected, considering that, as the negative

charge of the triflate ion is delocalized on the SO_3 end, the latter group should in principle bond preferentially to the cation.

The main conclusion that stems from the spectroscopic study performed here is that the charge carriers of the d-U(2000)$_n$$LiCF_3SO_3$ di-ureasil system with the highest ionic conductivity (i.e., the sample with n = 20) must be very likely "free" anions or weakly coordinated species.

Conclusions

In this paper studies of the structural, morphology and electrochemical properties of a series of hybrid materials (di-ureasils) based on a host matrix composed of short POE chains covalently bonded to a siloxane backbone through urea groups and incorporating $LiCF_3SO_3$ are reported. Samples with $\infty \geq n > 1$ are amorphous. A crystalline POE/$LiCF_3SO_3$ complex was detected by FT-IR in the materials with $n \leq 10$. The conductivity maximum of this POE/siloxane system is found at n = 20 (5.8×10^{-6} $\Omega^{-1}cm^{-1}$ at RT). The electrochemical stability domain of this material spans 4.1 V. Although the carbonyl oxygen atoms of the urea groups of the di-ureasils interact with the alkali metal cations in the whole range of salt concentration examined,[46] we found spectroscopic evidences that coordination of the Li^+ ions to the ether oxygen atoms of the POE chains is restricted to samples with $n \leq 10$. However it is likely that the latter value is situated at slightly lower salt concentration. In all the samples investigated "free" triflate ions and weakly coordinated anionic species were detected. In the di-ureasils with $n \leq 40$ ions pairs ($Li^+CF_3SO_3^-$) or negatively charged triplets ($[Li(CF_3SO_3)_2]^-$) are formed. At $n \leq 5$ positively charged triplets ($[Li_2(CF_3SO_3)]^+$) also appear. Divalent positively charged multiplets $[Li_3(CF_3SO_3)]^{2+}$ are formed only at n = 1. The charge carriers of the d-U(2000)$_{20}$$LiCF_3SO_3$ conductivity maximum appear to be "free" anions or weakly coordinated species.

The encouraging results obtained with the d-U(2000)$_n$LiCF$_3$SO$_3$ nanocomposites, in particular the improved mechanical properties and the moderate ionic conductivity, induce us to state that further research on Li^+-doped d-U(2000)-based di-ureasils is fully justified. The incorporation of a more suitable third generation lithium salt instead of LiCF$_3$SO$_3$ will certainly permit us to obtain materials with higher ionic conductivity values.

This work was supported by Fundação para a Ciência e Tecnologia (POCTI/P/CTM/33653/00, SFRH/BD/13559/03 and POCTI/P/CTM/46780/03). S. C. Nunes acknowledges Fundação para a Ciência e Tecnologia for a grant. D. Ostrovskii thanks National Research Council (Sweden) for financial support. The authors thank A. P. Passos de Almeida for her help in the DSC measurements.

References

1. P. V. Wright, *Br. Polymer*, **7**, 319 (1975)

2. M. Armand, M. T. Duclot and J. M. Chabagno, in Proceedings of the Second International Meeting on Solid State Electrolytes, St. Andrews, Scotland (1978), Extended Abstract 6.5

3. F. M. Gray, Polymer Electrolytes, RSC Materials Monographs, The Royal Society of Chemistry, London (1997)

4. J.-M. Tarascon and M. Armand, *Nature*, **414**, 359 (2001)

5. C. Berthier, W. Gorecki, M. Minier, M. B. Armand, J. M. Chabagno and P. Rigaud, *Solid State Ionics*, **11**, 91 (1983)

6. Z. Gadjourova, Y. G. Andreev, D. P. Tunstall and P. G. Bruce, *Nature*, **412**, 520 (2001)

7. C. J. Brinker and G. W. Scherer, Sol-gel Science: The Physics and Chemistry of Sol-Gel Processing, Academic Press, San Diego, CA (1990)

8. Functional Hybrid Materials, P. Gomez-Romero and C. Sanchez, Editors, Wiley Interscience, New York, (2003)

9. D. Ravaine, A. Seminel, Y. Charbouillot and M. Vincens, *J. Non-Cryst. Solids*, **82**, 210 (1986)

10. M. Popall, M. Andrei, J. Kappel, J. Kron, K. Olma and B. Olsowski, *Electrochim. Acta*, **43 (10-11)**, 1155 (1998)

11. P. Judeinstein, J. Titman, M. Stamm and H. Schmidt, *Chem. Mater.*, **6**, 127 (1994)

12. K. Dahmouche, M. Atik, N. C. Mello, T. J. Bonagamba, H. Panepucci, M. A. Aegerter and P. Judeinstein, *J. Sol-Gel Sci. Technol*., **8**, 711 (1997)

13. V. de Zea Bermudez, L. Alcácer, J. L. Acosta and E. Morales, *Solid State Ionics*, **116**, 197 (1999)

14. C. Wang, Y. Wei, G. R. Ferment, W. Li and T. Li, *Mater. Lett*., **39**, 206 (1999)

15. J. R. MacCallum and S. Seth, *Eur. Polym. J*., **36**, 2337 (2000)

16. K. Nishio and T. Tsuchiya, *Sol. Energy Mater. Sol. Cells*, **68**, 295 (2001)

17. M. Armand, C. Poinsignon, J.-Y. Sanchez and V. de Zea Bermudez, U.S. Patent 5, 283, 310, 1993

18. V. de Zea Bermudez, C. Poinsignon and M. B. Armand*, J. Mater. Chem*., **7(9)**, 1677 (1997)

19. V. de Zea Bermudez, D. Baril, J.-Y. Sanchez, M. Armand and C. Poinsignon, A. Hugot-Le Goff, C.- G. Granqvist and C. M. Lampert, Editors, Proc. SPIE, 1992, Vol. 1728, pág. 180

20. M. M Silva, V. de Zea Bermudez, L. D. Carlos, A. P. Passos de Almeida and M. J. Smith, *J. Mater. Chem*., **9**, 1735 (1999)

21. M. M. Silva, V. de Zea Bermudez, L. D. Carlos and M. J. Smith, *Electrochim. Acta*, **45**, 1467 (2000)

22. PeakFit is a product of Jandel Corporation, 2591 Rerner Boulevard, San Rafael, CA 94901, U.S.A.

23. F. Ribot, A. Lafuma, C. Eychenne-Baron and C. Sanchez, *Adv. Mater.,* **14**, 1496 (2002)

24. D. Cohn, A. Sosnik and A. Levy, *Biomater*., **24**, 3707 (2003)

25. M. C. Gonçalves, V. de Zea Bermudez, R. A. Sá Ferreira, L. D. Carlos, D. Ostrovskii and J. Rocha, *Chem. Mater*., in press

26. S. R. Davis, A. R. Brough and A. Atkinson, *J. Non-Cryst. Solids*, **315**, 197 (2003)

27. A.-C. Franville, D. Zambon, R. Mahiou and Y. Troin, *Chem. Mater.*, **12**, 428 (2000)

28. T. C. Chang, G. P. Wang, H. C. Tsai, Y. S. Hong and Y. S. Chiu, *Polym. Degrad. Stab.* **74**, 229 (2001)

29. E. El Nahhal, M. M. Chehimi, C. Cordier and G. Dodin, *J. Non-Cryst. Solids*, **275**, 142 (2000)

30. S. Hvidt, E. B. Jørgersen, W. Brown and K. Schillén, *J. Phys. Chem*., **98**, 12320 (1994)

31. E. A. Williams, C. L. Sabourin, P. E. Donahue, J. L. Spivack and N. A. Marotta, General Electric Research & Development Center, Technical Information Series (98CRD171), Dec. 1998

32. L. D. Carlos, R. A. Sá Ferreira, I. Orion, V. de Zea Bermudez and J. Rocha, *J. Lumin.* **87-89**, 702 (2000)

33. L. D. Carlos, V. de Zea Bermudez, R. A. Sá Ferreira, L. Marques and M. Assunção, *Chem. Mater*., **11(3)**, 581 (1999)

34. C. D. Robitaille and D. Fauteux*, J. Electrochem. Soc*., **133(2)**, 315 (1986)

35. S. M. Zahurak, M. L. Kaplan, E. A. Rietman, D. W. Murphy and R. J. Cava, *Macromolecules*, **21**, 654, (1988)

36. A. Vallée, S. Besner and J. Prud'homme, *Electrochim. Acta*, **37(9)**, 1579, (1992)

37. C. P. Rhodes and R. Frech, *Macromolecules*, **34**, 2660 (2001)

38. P. G. Bruce, S. A. Campbell, P. Lightfoot and M. A. Mehta, *Solid State Ionics*, **78**, 191 (1995)

39. P. Rigaud, Ph.D. Thesis, University of Grenoble, France, 1980

40. B. L. Papke, R. Dupon, M. A. Ratner and D. F. Shriver, *Solid State Ionics*, **5**, 685 (1981)

41. B. L. Papke and M. A. Ratner, D. F. Shriver, *J. Electrochem. Soc.*, **129(7)**, 1434 (1982)

42. A. Bernson, J. Lindgren, W. Huang and R. Frech, *Polym.*, **36(23)**, 4471 (1995)

43. K. Machida and T. Miyazawa, *Spectrochim. Acta*, **20**, 1865 (1964)

44. H. Matsuura and T. Miyazawa, *J. Polym. Sci*., **7(A-2)**, 1735 (1969)

45. M. A. K. L. Dissanayake and R. Frech, *Macromolecules*, **28(**15), 5312 (1995)

46. S. C. Nunes, V. de Zea Bermudez, D. Ostrovskii and L. D. Carlos, *J. Mol. Struct.*, in press

47. Å. Wendsjö, J. Lindgren, J. O. Thomas and G. C. Farrington, *Solid State Ionics*, **53-56**, 1077 (1992)

48. A. Bernson and J. Lindgren, *Solid State Ionics*, **60**, 37 (1993)

49. W. Huang, R. Frech and R. A. Wheeler, *J. Phys. Chem*., **98**, 100 (1994)

50. D. H. Johnston and D. F. Shriver, *Inorg. Chem*. **32**, 1045 (1993)

51. J. R. Stevens and P. Jacobsson, *Can. J. Chem*., **69**, 1980 (1991)

52. L. M. Torell, P. Jacobsson and G. Petersen, *Polym. Adv. Tech*., **4**, 152 (1992)

53. P. Jacobsson I. Albisson, B.-E. Mellander and J. R. Stevens, *Polym*., **33(13)**, 2778 (1992)

54. G. Petersen, L. M. Torell, S. Panero, B. Scrosati, C. J. Silva and M. J. Smith, *Solid State Ionics*, **60**, 55 (1993)

55. G. Petersen, A. Brodin, L. M. Torell and M. J. Smith, *Solid State Ionics*, **72**, 165 (1994)

56. A. Brodin, B. Mattsson, K. Nilsson, L. M. Torrel and J. Hamara, *Solid State Ionics*, **85**, 111 (1996)

57. R. Frech, S. Chintapalli, P. G. Bruce and C. A. Vincent, *Chem. Comm*., 157 (1997)

58. R. Frech, S. Chintapalli, P. G. Bruce and C. A. Vincent, *Macromolecules*, **32**, 808 (1999)

59. V. de Zea Bermudez, D. Ostrovskii, S. Lavoryk, M. C. Gonçalves and L. D. Carlos, *Phys. Chem. Chem. Phys.*, **6(3)**, 649 (2004)

60. M. C. Gonçalves, V. de Zea Bermudez, D. Ostrovskii and L. D. Carlos, *Electrochim. Acta*, **48**, 1977 (2003)

61. M. C. Gonçalves, V. de Zea Bermudez, D. Ostrovskii and L. D. Carlos, *Solid State Ionics*, **166(1-2)**, 103 (2004)

List of figure captions

Figure 1 - ^{13}C CP/MAS (a) and ^{29}Si MAS (b) NMR spectra of selected d-U(2000)$_n$LiCF$_3$SO$_3$ di-ureasils

Figure 2 - XRD patterns of selected d-U(2000)$_n$LiCF$_3$SO$_3$ di-ureasils

Figure 3 - Thermal behaviour of selected d-U(2000)$_n$LiCF$_3$SO$_3$ di-ureasils: (a) DSC thermograms; (b) Glass transition temperature versus composition (Note: the line drawn is just a guide for the eyes); (c) TGA curves.

Figure 4 - Arrhenius conductivity plot (a) and isotherms of the ionic conductivity versus composition (b) of the d-U(2000)$_n$LiCF$_3$SO$_3$ di-ureasils

Figure 5 - RT cyclic voltamogram of the d-U(2000)$_{20}$LiCF$_3$SO$_3$ di-ureasil (5^{th} cycle, sweep rate = 10 mV s^{-1}) obtained with a stainless steel working electrode and lithium counter and reference electrodes.

Figure 6 - RT FT-IR spectra (a) and curve-fitting results ((b) and (c)) of selected d-U(2000)$_n$LiCF$_3$SO$_3$ di-ureasils in the νCO region. The wavenumbers indicated in (a) and (c) regard the values observed in the spectrum of the most concentrated sample.

Figure 7 - RT FT-Raman spectra (a) and curve-fitting results (b) of selected d-U(2000)$_n$LiCF$_3$SO$_3$ di-ureasils in the $\nu_s SO_3$ region. In order to examine exclusively the contribution of the $\nu_s SO_3$ mode, the FT-Raman spectrum of the pure polymer had to be first subtracted from those of the hybrids with $n \geq 10$.

Figure 8 - RT FT-Raman spectra (a) and curve-fitting results (b) of selected d-U(2000)$_n$LiCF$_3$SO$_3$ di-ureasils in the $\delta_s CF_3$ region.

Tables

Table 1 - NMR data (in ppm) of the d-UPTES(2000) precursor and of selected d-U(2000)$_n$LiCF$_3$SO$_3$ di-ureasils

Table 2 - Relevant details of the synthetic procedure of the d-U(2000)$_n$LiCF$_3$SO$_3$ di-ureasils

Scheme

Scheme 1 - Structure of the d-UPTES(2000) di-ureasil precursor

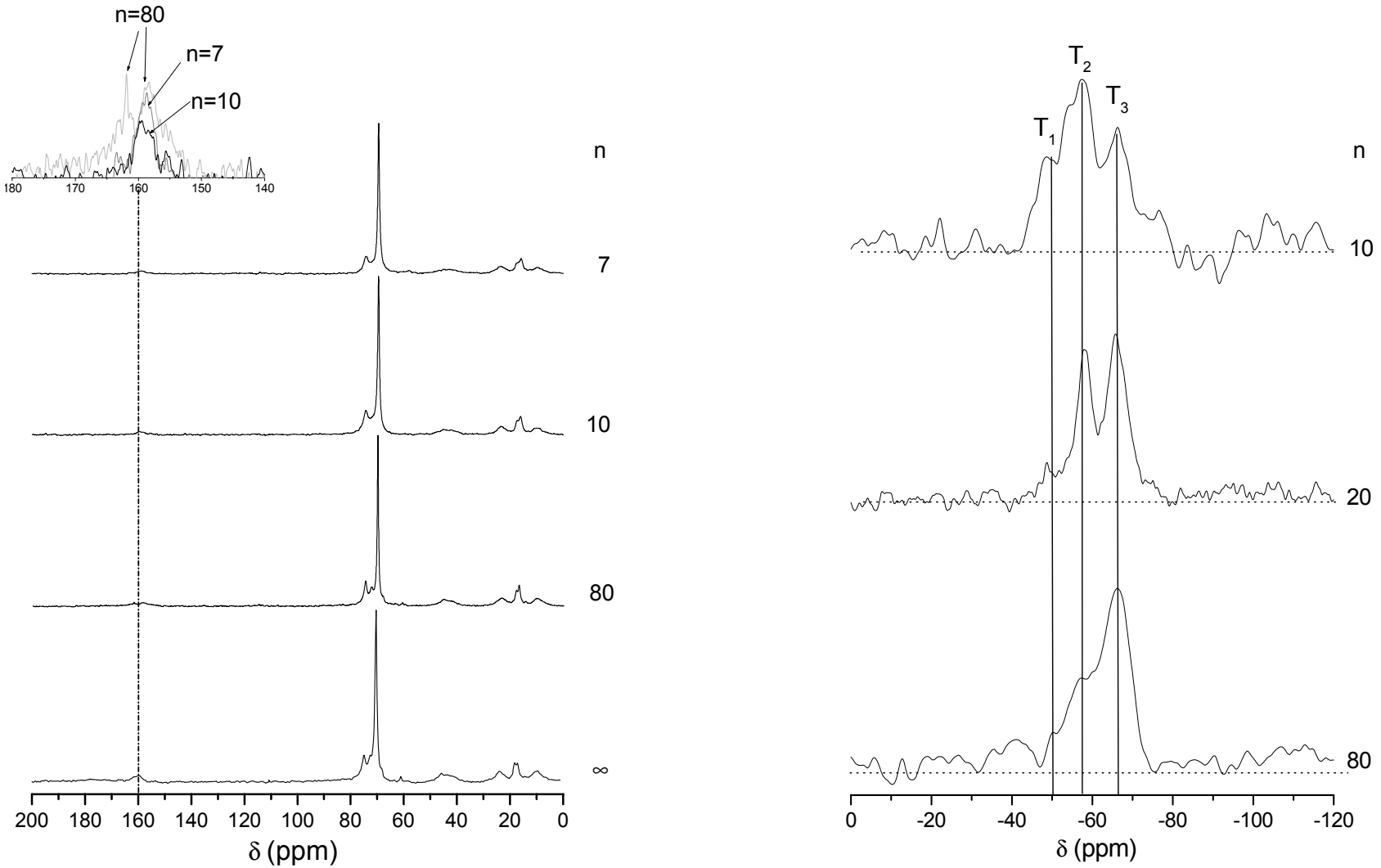

(a) (b)

Figure 1, S. C. Nunes et al., J. Electrochem. Soc.

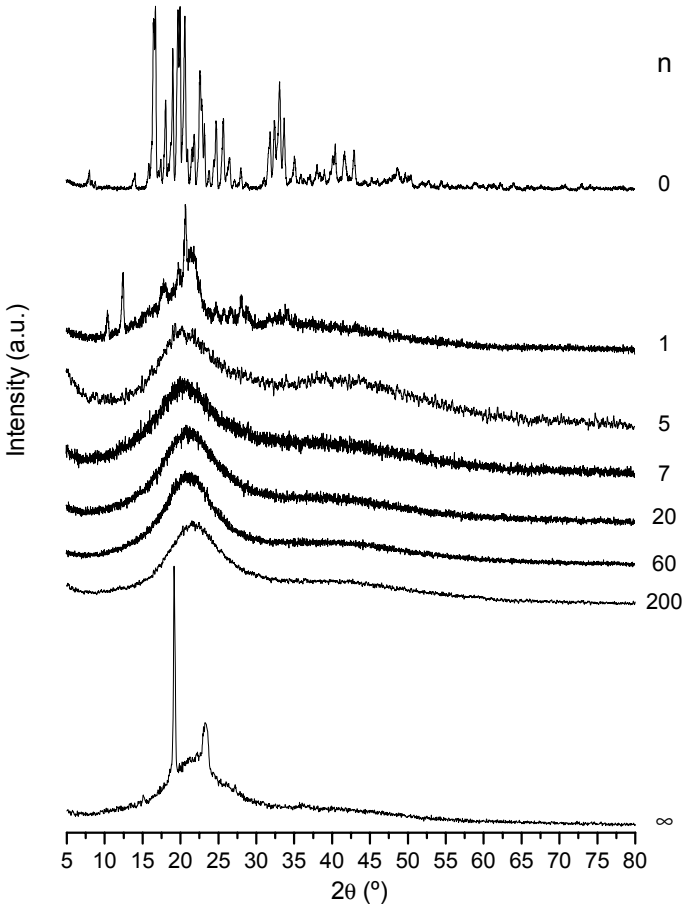

Figure 2, S. C. Nunes et al., J. Electrochem. Soc.

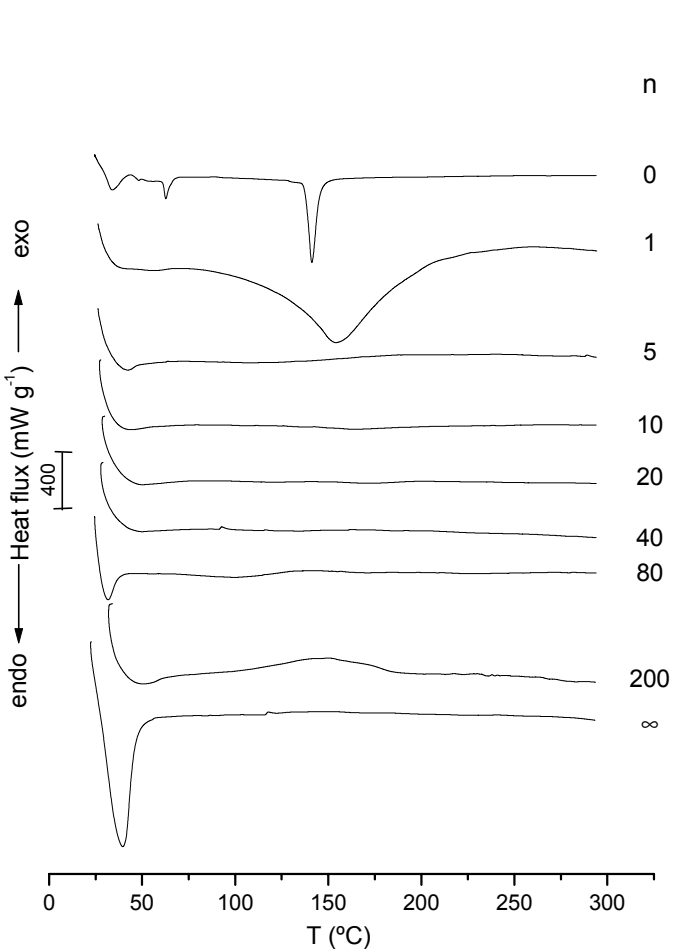

(a)

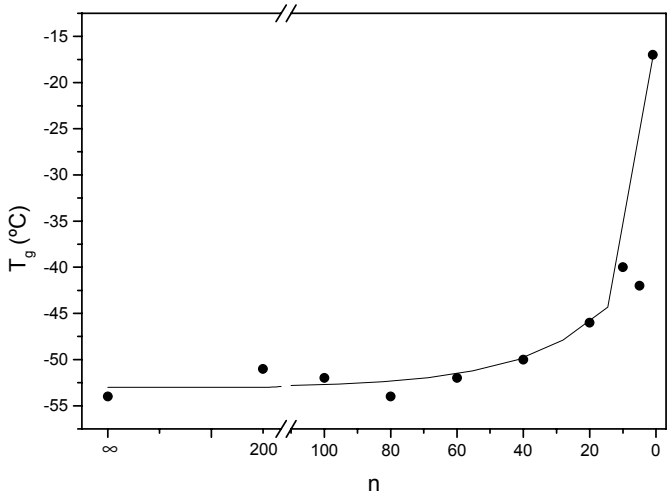

(b)

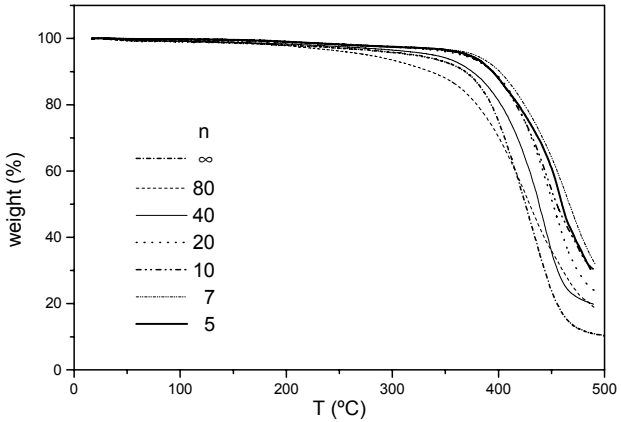

(c)

Figure 3, S. C. Nunes et al., J. Electrochem. Soc.

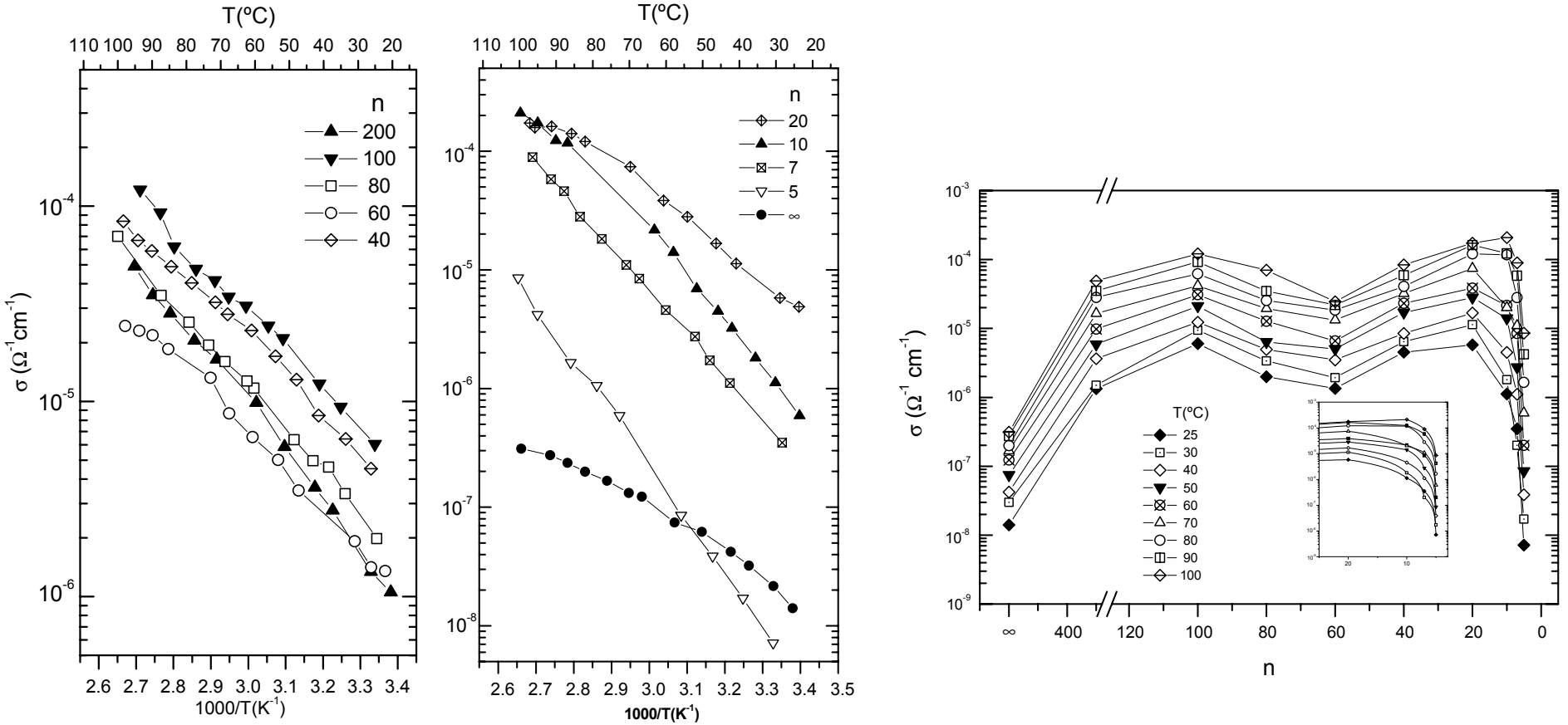

(a) (b)

Figure 4, S. C. Nunes et al., J. Electrochem. Soc.

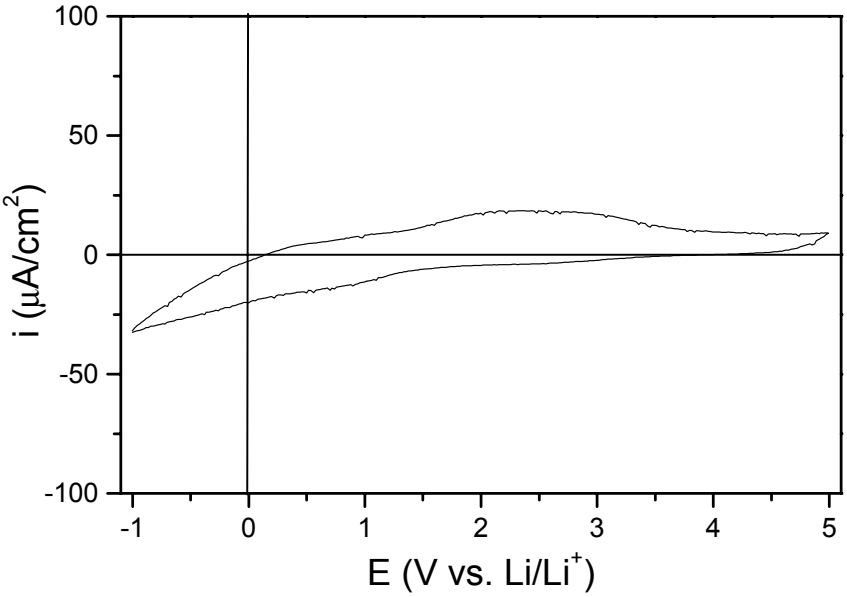

Figure 5, S. C. Nunes et al., J. Electrochem. Soc.

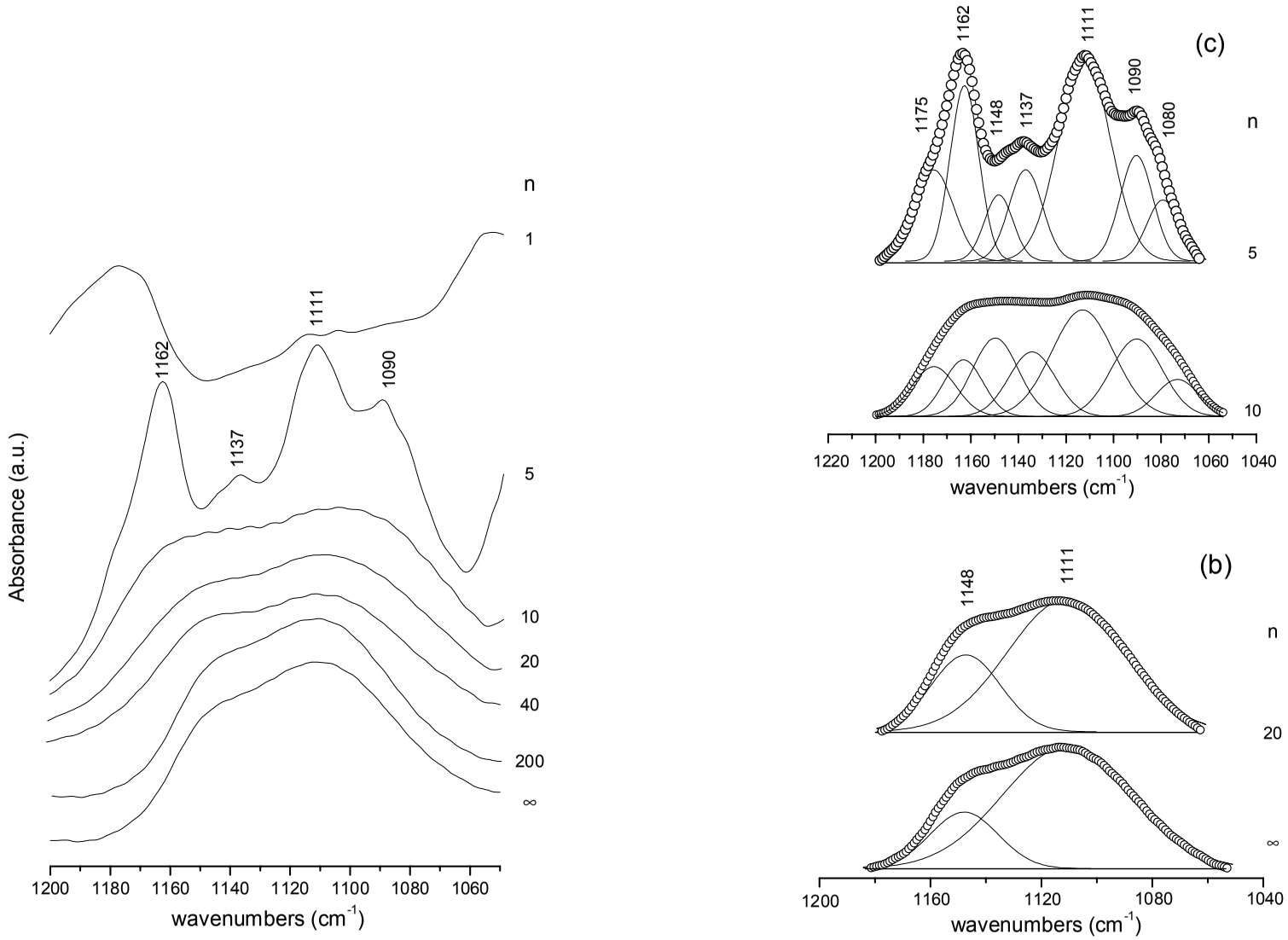

Figure 6, S. C. Nunes et al., J. Electrochem. Soc.

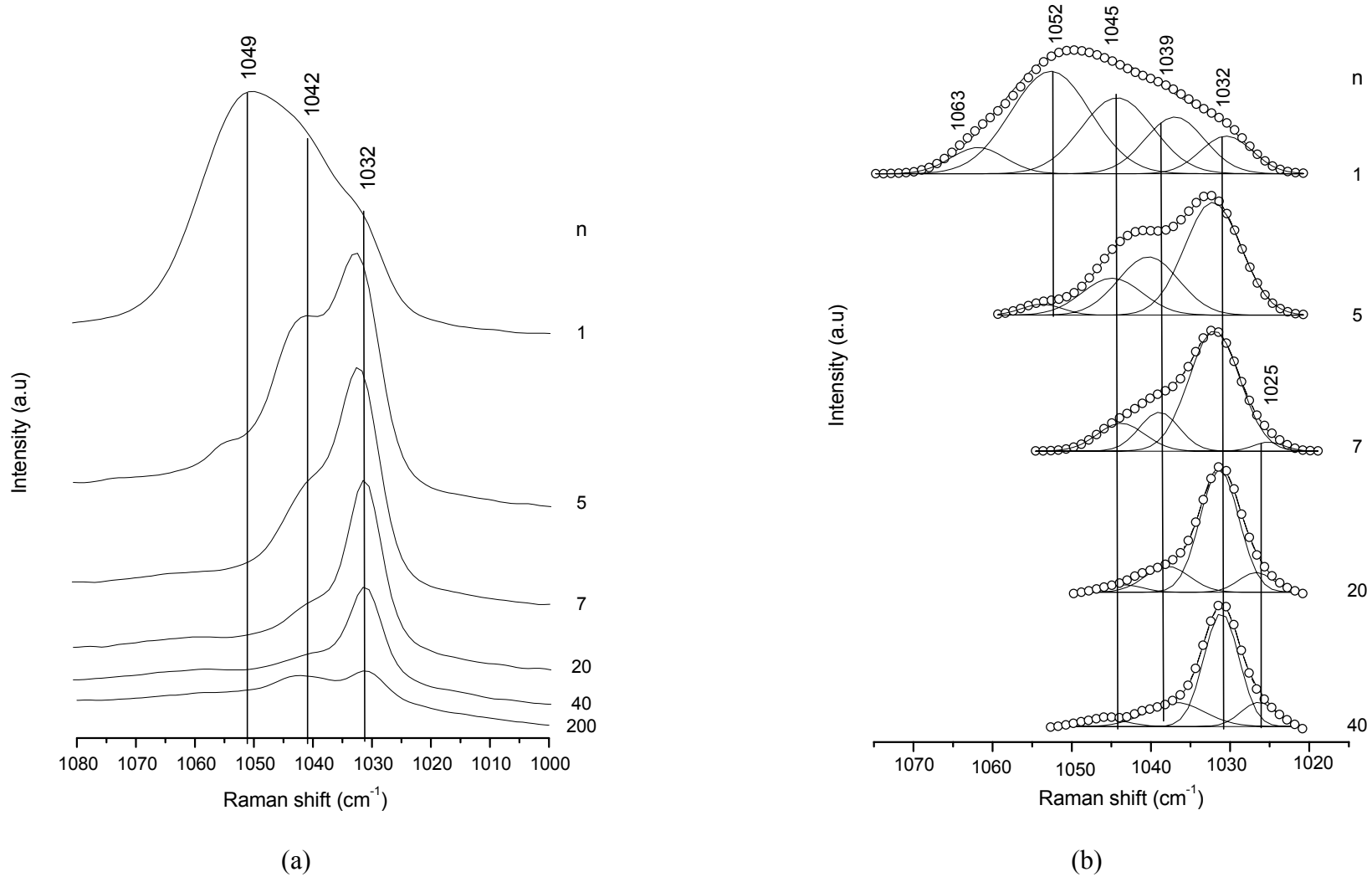

(a) (b)

Figure 7, S. C. Nunes et al., J. Electrochem. Soc.

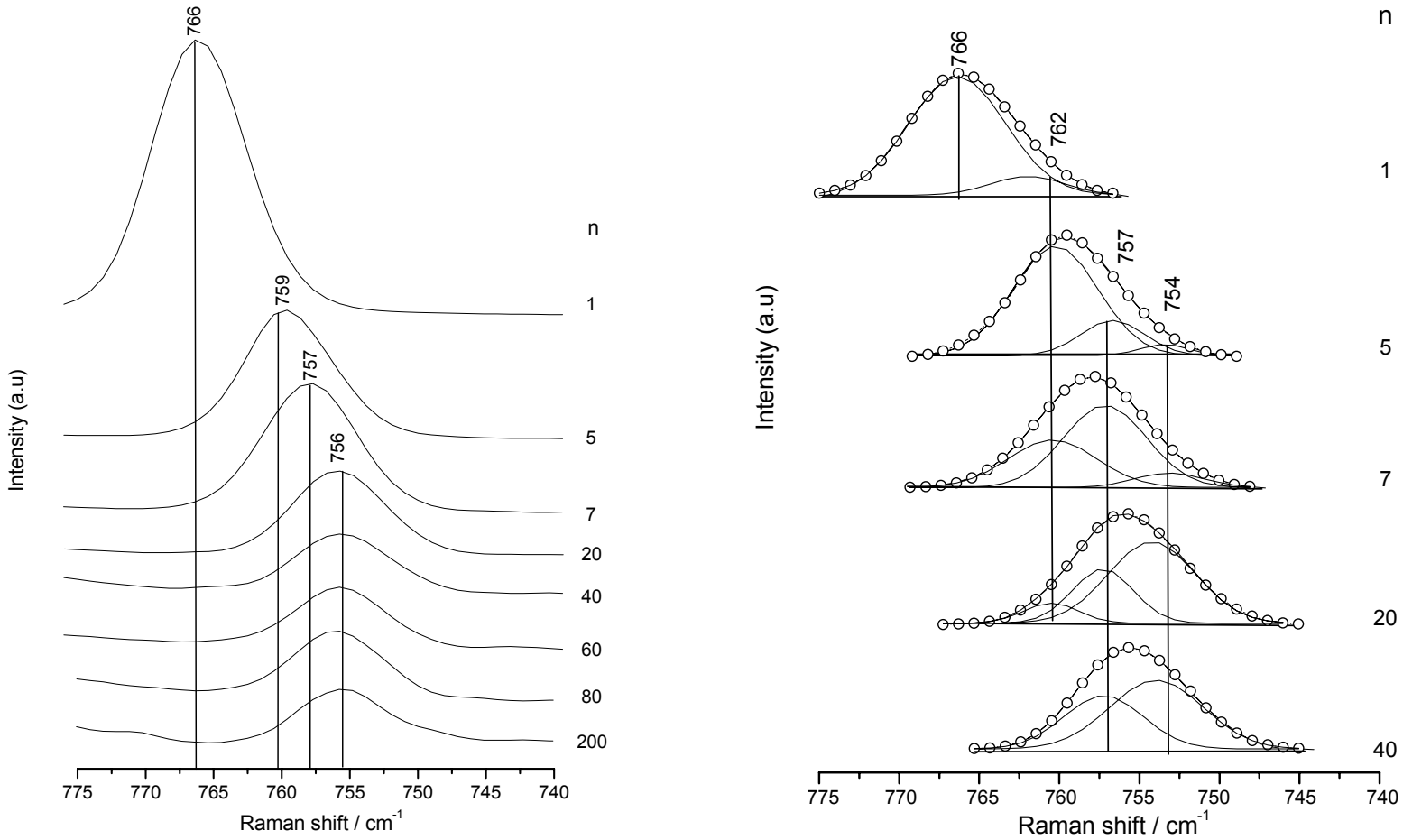

(a) (b)

Figure 8, S. C. Nunes et al., J. Electrochem. Soc.

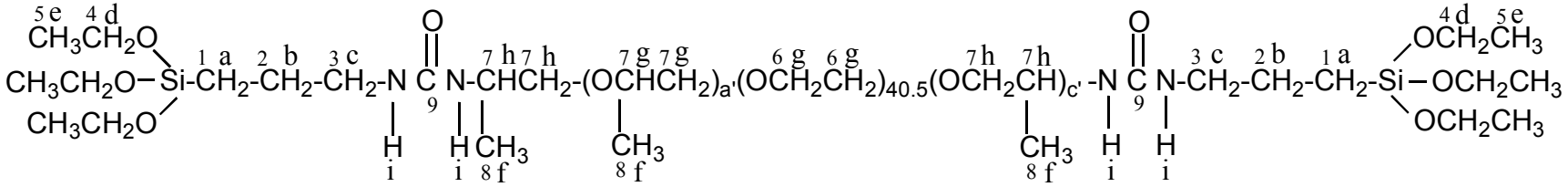

Scheme 1, S. C. Nunes et al, J. Electrochem. Soc.

Table 1, S. C. Nunes et al., J. Electrochem. Soc.

^{1}H NMR d-UPTES(2000)			Attribution[11,23-31]	^{13}C NMR d-UPTES(2000)	^{13}C CP/MAS NMR d-U(2000)$_n$LiCF$_3$SO$_3$				Attribution[11,23-31]
					∞	80	10	7	
3.92-3.82	m	12H	H^d	158.19	160	-	-	-	C^9
3.79-3.51	m	≈162H	H^g	77.32-74.88	75	75	-	-	C^7
3.49-3.29	m	≈11H	H^h	73.12-70.11	72-70	70	70	70	C^6
3.20-3.04	m	4H	H^c	58.30-58.14	61	61	61	-	C^4
2.38	s,b	4H	H^i	42.72	47-41	-	-	-	C^3
1.56-1.51	m	4H	H^b	23.75-23.53	25-22	-	-	-	C^2
1.18-1.15	m	18H	H^e	18.32-18.21	18	18	18	-	C^5
1.12-1.02	m	18H	H^f	17.04-16.78	17	-	-	-	C^8
0.60-0.55	m	4H	H^a	7.60-7.50	15-10	-	-	-	C^1

^{29}Si MAS NMR

n	T_1 (CH_2-Si(OSi)(OR)$_2$) population (%)		T_2 (CH_2-Si(OSi)$_2$(OR)) population (%)		T_3 (CH_2-Si(OSi)$_3$) population (%)		c (%)	Empirical formula
80	-50.0	1.1	-58.3	43.0	-66.6	55.9	85	$R'_{0.5}Si(OR)_{0.45}(O)_{1.3}$
20	-53.0	1.4	-58.1	37.2	-66.0	61.4	87	$R'_{0.5}Si(OR)_{0.4}(O)_{1.3}$
10	-49.2	23.3	-56.5	29.1	-65.6	47.6	75	$R'_{0.5}Si(OR)_{0.76}(O)_{1.1}$

Note: R'= -$(CH_2)_3$-NH-C(=O)-NH-(CH(CH_3)CH_2-(OCH(CH_3)CH_2)$_a$-(OCH_2CH_2)$_{40.5}$-(OCH(CH_3)CH_2)$_b$-NH-C(=O)-NH-$(CH_2)_3$-

R = H ou CH_2CH_3; m – multiplet, s – singlet and b - broad

Table 2, S. C. Nunes et al., J. Electrochem. Soc.

$n = O/Li^+$ (mol / mol)	$m(LiCF_3SO_3)$ (g)	Si/Li^+ (mol / mol)	Si/Li^+ (g / g)
∞	-	-	-
200	0.0395	9.8765	15.6603
100	0.0790	4.9383	7.8301
80	0.0987	3.9506	6.2641
60	0.1316	2.9630	4.6981
40	0.1974	1.9753	3.1321
20	0.3949	0.9876	1.5660
10	0.7898	0.4938	0.7830
5	1.5796	0.2469	0.3915
1	7.8980	0.0494	0.0783